

Modeling Jump Diffusion in Zeolites: II. Applications[†]

Scott M. Auerbach

Department of Chemistry and Department of Chemical Engineering

University of Massachusetts, Amherst, MA 01003 USA

Abstract

We review recent applications of jump models for diffusion in zeolites. We describe the results of a coarse-grained model of the interplay between zeolite anisotropy and disorder, finding that certain disorder patterns can change how anisotropy controls membrane permeation. We show the results of a lattice model for single-file diffusion in zeolite membranes, demonstrating how single-file motion is manifested in anomalous mean-square displacements at short times, and in non-intensive Fickian self-diffusion coefficients at later times. We discuss a normal-mode analysis approach for treating framework flexibility for tight-fitting zeolite-guest systems, showing that simulations allowing for framework flexibility can converge in *less CPU time* than those that keep the framework rigid. We then explore models of the loading dependence of self-diffusion in zeolites, with emphasis on benzene in NaX and NaY. We enumerate the decisions that need to be made when modeling such systems, and indicate the choices/approximations we have made for modeling benzene in NaX and NaY. We report kinetic Monte Carlo results for the loading dependence of benzene diffusion in NaX, which is found in reasonable agreement with NMR data, but in poor agreement with tracer ZLC results. We then speculate on the possibility of having a subcritical fluid adsorbed in a nanoporous material, and how such a thermodynamic state would impact diffusion in such a system. We close with a review of outstanding problems in modeling jump diffusion in zeolites.

[†]Submitted for the *Proceedings of the NATO Advanced Study Institute* on “Fluid Transport in Nanopores,” Eds. J. Fraissard, W.C. Conner, Jr., and V. Skirda, La Colle Sur Loup, France, June 16-27, 2003.

1. Introduction

In our preceding chapter, we introduced the main ideas necessary to understand jump diffusion in zeolites. Here we bring these ideas to life with some examples studied by Auerbach and coworkers.

2. Modeling the Interplay between Non-Zeolitic Voids and Anisotropy

Zeolite membranes exhibit two structural features that can conspire to produce novel transport properties; these are anisotropy and non-zeolitic voids. Structural anisotropy is particularly important for zeolites, and takes on even more importance when considering, e.g., *para*-xylene motion in an MFI-type zeolite (Figure 1), where motion along the straight channel is expected to be much faster than in other directions. Unfortunately, most MFI membranes are not as “simple” as that. Figure 2 shows a scanning electron micrograph (SEM) of an MFI membrane cross-section, showing clear evidence of grain boundaries and non-zeolitic voids in the heart of the membrane [1]. The question is: what is the interplay between such anisotropy and non-zeolitic voids on fluid transport through nanoporous membranes?

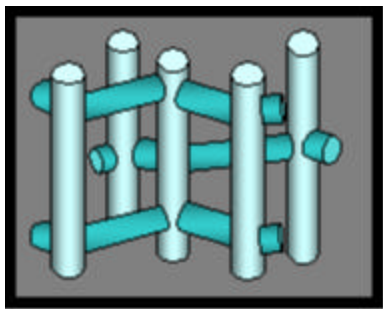


Figure 1: MFI structure cartoon.

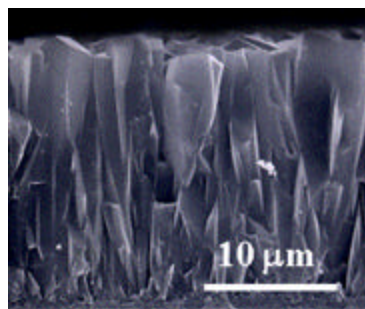


Figure 2: SEM of C-oriented MFI.

To address this issue, Nelson *et al.* developed a finite-difference formulation of Fick’s diffusion equation for use with the model membrane system shown in Figure 3 [1]. Details of the calculations can be found in Ref. [1].

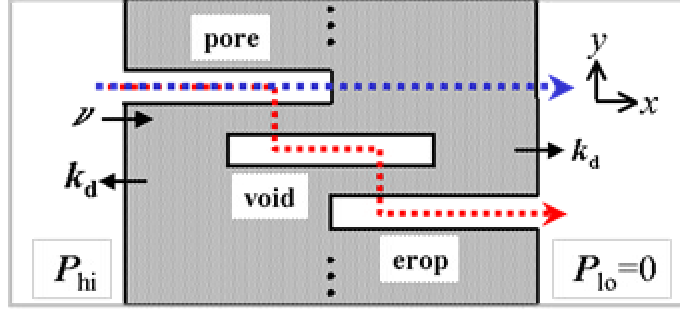


Figure 3: Model with pore, void and erop, and with straight and short-cut pathways.

We wish to determine how steady-state fluxes vary with anisotropy and void properties. In particular, it is interesting to wonder whether transport through the void in Figure 3 (i.e. “short-cut” flux) can compete with transport that avoids the void. We define an anisotropy parameter $\mathbf{h} = k_y/k_x = D_y/D_x$, which is the ratio of site-to-site jump rates in the in-plane (k_y) and trans-membrane (k_x) directions, and is also the ratio of self-diffusivities in these directions. In general, the anisotropy depends on temperature because k_x and k_y are determined by different activation energies. In terms of these microscopic inputs, the finite-difference equations take the form:

$$\begin{aligned} \frac{d\mathbf{q}_{x,y}}{dt} = & \frac{D_x}{(dx)^2}(\mathbf{q}_{x-1,y} - \mathbf{q}_{x,y}) + \frac{D_x}{(dx)^2}(\mathbf{q}_{x+1,y} - \mathbf{q}_{x,y}) \\ & + \frac{D_y}{(dy)^2}(\mathbf{q}_{x,y-1} - \mathbf{q}_{x,y}) + \frac{D_y}{(dy)^2}(\mathbf{q}_{x,y+1} - \mathbf{q}_{x,y}) \end{aligned}$$

where dx and dy are grid spacings. Edge-site fluxes are replaced with terms involving ν , the insertion-attempt frequency per edge site, and k_d , the rate coefficient controlling activated desorption from edge sites.

We seek to determine how steady-state flux depends on anisotropy for membranes with defects. The flux also depends on temperature; here we quote the maximum possible flux for a given set of input parameters. Figure 4 shows the peak flux, J_{\max} , as a function of diffusion anisotropy for two values of the

distance between defects, Δy . Because the diffusion anisotropy varies with temperature, we plot J_{\max} against the value of h at the temperature T_{\max} , corresponding to the maximum flux.

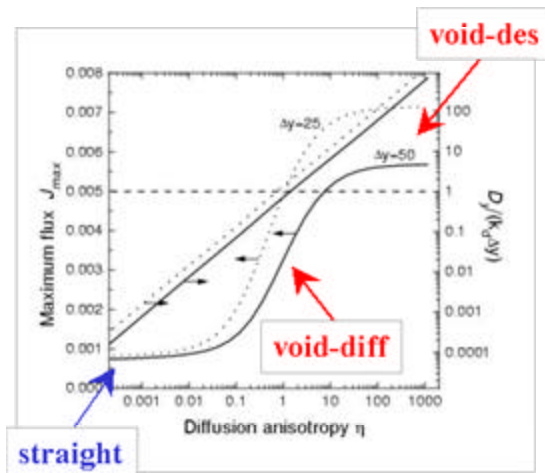


Figure 4: Peak flux (J_{\max}) vs. diffusion anisotropy (h) for membranes with voids.

Three regimes can be identified in Figure 4: (i) diffusion-limited along the x -direction for low h values; (ii) diffusion-limited along the y -direction for intermediate h values; (iii) sorption-limited along the y -direction for large h values. Indeed, at low values of the anisotropy, diffusion in the y -direction is slowed down dramatically and transport through the shortcut becomes negligible. As a result, the peak flux approaches a constant value for small h . This constant flux is related to the average length of defects along the x -direction. At intermediate values of h , membrane permeation through the short cut begins to dominate, producing peak flux that grows with h . This indicates that membrane permeation is controlled by the rate of diffusion from pore to void to erop, i.e., along the y -direction. When h becomes even larger, motion from pore to void to erop is no longer limited by diffusion, but rather by the rate of desorption into the void. In this case, the peak flux becomes independent of h , precisely because membrane permeation is no longer limited by diffusion along the y -direction.

As a concrete example to illustrate the importance of these results, several research groups have endeavored to synthesize b -oriented silicalite membranes with the expectation that permeating molecules

will diffuse primarily down the straight channels. While there has been remarkable success reported in synthesizing oriented silicalite membranes, most of these membranes still suffer from many defects such as grain boundaries and non-zeolitic voids. Our results show that, with certain defect patterns and diffusion anisotropies, it is entirely possible that membrane permeation can be controlled by motion along the zig-zag channels of silicalite, even when the membrane is oriented with the straight channels parallel to the trans-membrane axis. That is because motion through the zig-zag channels may carry molecules from pore to void to erop faster than that possible by motion exclusively through straight channels. Zeolite scientists who make membranes may have to strike a balance between synthesizing membranes that are sufficiently oriented and sufficiently defect-free.

3. Modeling Single-File Diffusion in Zeolites of Finite Length

In the limit of vanishing diffusion anisotropy, $\mathbf{h} \rightarrow 0$, one-dimensional or so-called single-file diffusion dominates transport. For transport down a gradient, single-file diffusion obeys the usual equations of Fickian theory. On the other hand, for self-diffusion under equilibrium conditions, single-file diffusion suffers from such strong vacancy correlations (see previous chapter by Ramanan and Auerbach) that the phenomenology changes. In particular, the mean-square displacement (MSD) for single-file self-diffusion takes the anomalous form $\langle x^2 \rangle = 2Ft^{1/2}$, as opposed to the normal linear dependence in the Einstein equation; here F is denoted the single-file mobility. This $t^{1/2}$ dependence was predicted by theory for infinitely long files [2]. However, all *real* files are finite in extent. Thus, we wonder how single-file self-diffusion is influenced by the finite extent of real files.

To explore this, Nelson and Auerbach performed open-system kinetic Monte Carlo (KMC) simulations on the system pictured in Figure 5 [3]. For details regarding these simulations, we refer the reader to Ref. [3]. Because self-diffusion involves the stochastic motion of tagged particles, we used KMC to evolve the motions of tagged particles in files with untagged particles. The entire system (tagged plus untagged particles) is at equilibrium, and all particles have identical diffusion and sorption properties.

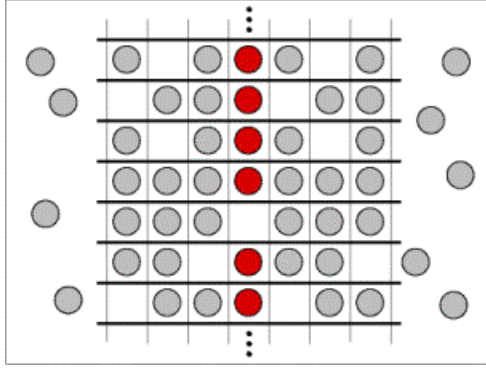


Figure 5: Simulation set-up to study single-file self-diffusion in files of finite extent.

Figure 6 shows a log-log plot of the resulting MSD. In such a log-log plot, the slope gives the exponent of time in the MSD, e.g., a slope of 1 indicates normal Fickian behavior. Here we see three regimes: (i) mean-field diffusion at very short times; (ii) anomalous $t^{1/2}$ behavior at intermediate times; (iii) at longer times a surprising return to Fickian behavior even though none of the tagged particles has desorbed from their files. The time in Figure 6 is measured in units of the average site-residence time, τ . At very short times, $t < \tau$, a particle is unlikely to feel its neighbor, and thus exhibits normal diffusion in the mean-field limit where the vacancy correlation factor is near unity. At longer times, $t > \tau$, highly-correlated collisions between neighboring sorbates confined in the single file yields anomalous diffusion. One might naively presume that such behavior will persist until tagged particles desorb from their files. However, Figure 6 shows a surprising return to Fickian behavior well before particles leave their files. We and others have shown that this cross-over occurs at the time $t_c = L^2/pD_0$, where L is the file length and D_0 is the infinite-dilution self-diffusion coefficient. This cross-over time is essentially the time required for vacancies to diffuse from one end of the file to the other. After this time, the file edges strongly influence motion, which can be pictured as normal diffusion of the center-of-mass of particles in each file [4]. We and others have shown that the self-diffusion coefficient for this compound motion scales inversely with file length, which can be viewed as a new kind of anomaly.

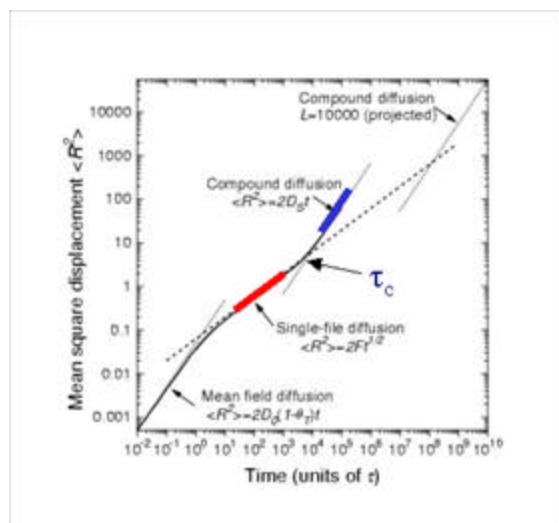


Figure 6: Log-log plot of MSD for tagged particles in finite single files.

This recurrence of Fickian motion with an anomalous self-diffusion coefficient alters somewhat the picture of single-file diffusion. We predict that the signature $t^{1/2}$ time-dependence of the MSD lasts for a relatively short time. Indeed, for a great majority of the lifetime inside a single-file, the tagged particles are found to exhibit Fickian transport with the anomalous self-diffusion coefficient. It is our contention that this provides the proper signature of single-file self-diffusion.

Observing this predicted recurrence of Fickian motion may be challenging for modern pulsed field gradient (PFG) NMR methods. PFG NMR is limited by spin-lattice relaxation, which significantly reduces signal-to-noise ratios. PFG NMR can usually measure motion for up to *ca.* 0.1 seconds. Assuming $L = 10 \mu\text{m}$ and $D_0 = 10^{-5} \text{ cm}^2/\text{sec}$, the cross-over time falls right around the maximum observation time for PFG NMR. Thus, testing the above simulation results may require the development of longer-time microscopic methods for measuring self-diffusion in zeolites.

4. Modeling Zeolite Flexibility in Rare-Event Dynamics

When guest molecules fit tightly in zeolite nanopores, transport through zeolites is dominated by jump diffusion. As shown below in Figure 7, benzene in silicalite provides an excellent example of such strong confinement. Snurr *et al.* applied harmonic transition state theory (TST) to benzene diffusion in

silicalite, assuming that benzene and silicalite remain rigid [5]. As a consequence of this assumption, their results underestimate experimental diffusivities by one to two orders of magnitude. Forester and Smith subsequently applied TST to benzene in silicalite using constrained reaction-coordinate dynamics on both rigid and flexible lattices [6]. Lattice flexibility was found to have a very strong influence on the jump rates. Diffusivities obtained from these (computationally demanding) flexible framework simulations are in excellent agreement with experiment, overestimating the measured room temperature diffusivity (2.2×10^{-14} m²/s) by only about 50%. These studies establish benzene in silicalite as an important benchmark system for which including framework flexibility is crucial for describing guest diffusion.

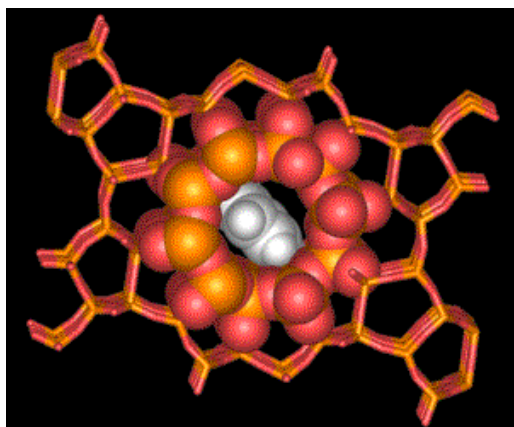


Figure 7: Benzene in silicalite's straight channel; example of tight fit.

Computing the fundamental site-to-site rate coefficients for such confined diffusion is challenging for the following reasons. First, guest diffusion is likely facilitated by peristaltic framework vibrations; simulating such vibrations requires the significant computational expense of a flexible-framework model. Second, peristaltic framework vibrations are highly cooperative motions, which are conveniently simulated using molecular dynamics (MD). Third, straightforward MD cannot be used to model the motions of strongly confined guests, whose site residence times are typically much longer than MD run times. These facts taken together make it challenging to find an efficient method for simulating strongly confined guest diffusion.

A solution to this problem was suggested by Turaga and Auerbach [7], following the normal-mode analyses of zeolite vibrations reported by Iyer and Singer [8]. They found that zeolite normal modes often correspond to breathing motions of rings and channels, suggesting that these coordinates can efficiently sample framework distortions during molecular jumps. What's more, a remarkable speedup can be obtained by exploiting the fact that zeolite vibrations are nearly harmonic, which has been established by Turaga and Auerbach. As such, after computing the normal modes, sampling lattice flexibility costs *essentially no CPU time* because the zeolite force constants are known. Thus, we use normal-mode coordinates for natural sampling of zeolite vibrations, and normal-mode force constants for efficient energy calculations. Below we show free energy surfaces for benzene jumping in silicalite's straight channel, finding excellent agreement with the results of Forester and Smith. However, in contrast with their calculations, the flexible-lattice simulations reported below converged in *less CPU time* than that required for fixed-lattice simulations.

The free energy landscape for benzene in silicalite is now reasonably well known, with relatively flat minima at intersection sites and corrugated regions of high free energy in channels. This landscape arises from a balance between the host-guest potential energy, host distortion energy and guest configurational entropy. Using the methods outlined above, Turaga and Auerbach calculated benzene's free energy surface (FES) along the crystallographic y -axis describing the jump between intersection sites, which are separated by about 10 Å. Results for flexible and rigid lattices are compared below in Figure 8. Both curves show the qualitative features indicated above. However, the rigid-lattice barrier is much higher than the flexible-lattice one, because the zeolite is allowed to distort during the latter simulations. Our flexible lattice FES is in excellent agreement with results of Forester and Smith. In agreement with their results, we find three shallow free-energy minima in the channel. Our barrier, 20 kJ/mol, is in very good agreement with their result, 25 kJ/mol, considering that slightly different forcefields were used. These results confirm that our local normal-mode Monte Carlo approach can faithfully represent molecular motion in tight-fitting zeolite-guest systems.

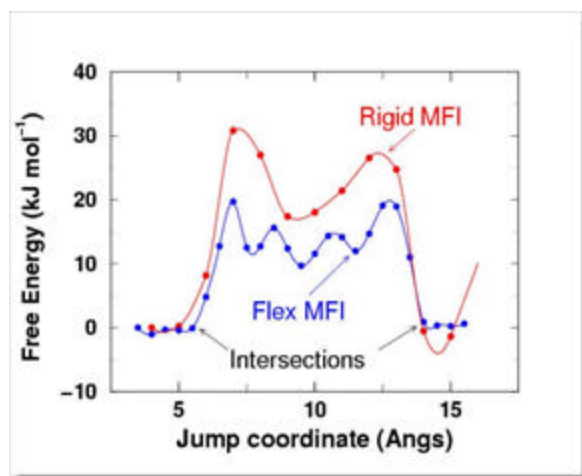


Figure 8: Free energy surface for benzene jumping in silicalite's straight channel.

For each flexible-lattice free energy in Figure 8, Turaga and Auerbach performed two Monte Carlo runs of length 10^6 steps (attempted moves). On the other hand, for each rigid-lattice free energy we performed two Monte Carlo runs of length ca. 10^7 steps. We note that the rigid-lattice FES does not reflect silicalite's symmetry along the reaction coordinate, while the flexible-lattice FES does. This indicates that, despite the longer Monte Carlo runs, the rigid-lattice FES remains more poorly converged than the flexible-lattice FES. This slow convergence occurs because of the decreased likelihood of jumping through a rigid lattice. A more efficient window sampling method might speed up the rigid-lattice FES convergence. Nonetheless, because the normal-mode algorithm makes rigid- and flexible-lattice calculations equally fast step for step, and our flexible calculations converged in fewer steps, we have shown that flexible-lattice calculations can actually be *faster* than rigid-lattice ones.

This algorithm will facilitate simulations of adsorption and diffusion in tight-fitting host-guest systems for hosts that behave as multi-dimensional harmonic oscillators during guest diffusion. This class of hosts includes most siliceous zeolites, many carbon nanotubes, and possibly the selectivity filters of biological ion channels. Exceptions include zeolites that undergo phase transitions upon guest adsorption, zeolites with exchangeable cations that diffuse alongside guests, biological ion pumps, and any host that executes large amplitude motion during guest diffusion.

5. Loading Dependence of Benzene Diffusion in FAU-type Zeolites

Several experimental and theoretical diffusion studies have been reported for benzene in NaX and NaY to help resolve persistent, qualitative discrepancies between experimental probes of the coverage dependence of self-diffusion. In particular, PFG NMR diffusivities decrease monotonically with loading [9], while tracer zero-length column (TZLC) data *increase* monotonically with loading [10]. The discrepancy between PFG NMR and TZLC casts doubt on using experimental self-diffusivities for designing processes in zeolites. Atomistic simulations, lattice models and field theories have been reported for this transport system. The simulations performed and methods employed have been reviewed in Refs. [11-13].

This discrepancy points to a larger problem: in general, we lack qualitative understanding how host-guest and guest-guest interactions conspire with thermal energies to produce different loading dependencies of self-diffusion. By analyzing PFG NMR diffusivities for many zeolite-guest systems, Kärger and Pfeifer reported five typical loading dependencies of self-diffusion [14], in analogy with the IUPAC designations for adsorption isotherms. Kärger and Pfeifer's results are shown schematically below in Figure 9. In 1999, Saravanan and Auerbach reported a lattice model of benzene diffusion in NaX, which yields diffusivities in agreement with PFG NMR data [15]. In addition, by varying fundamental energy parameters in their model, they found four of the five loading dependencies reported by Kärger and Pfeifer. Here we review the essential aspects of this work.

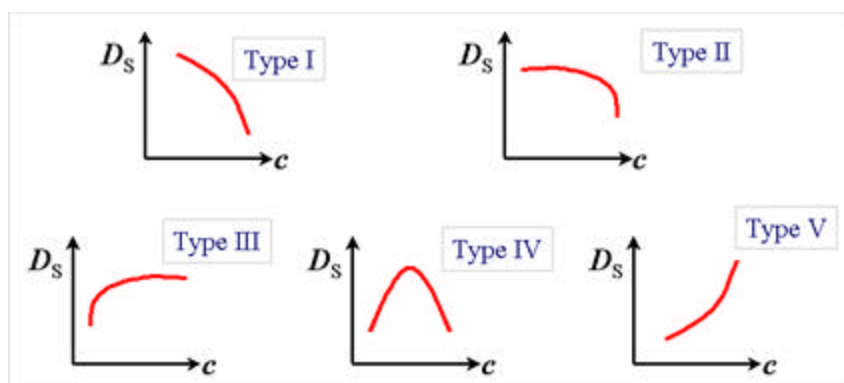


Figure 9: Kärger and Pfeifer's schematic loading dependencies of self-diffusion in zeolites.

When building a model of diffusion in zeolites at finite loadings, a variety of decisions must be made that impact the accuracy of the results and the efficiency of the computations. Below in Figure 10 we outline the typical decisions that need to be made, and underline the choices we have made in modeling benzene in NaX. Our model for benzene diffusion assumes that benzene molecules jump among S_{II} and W sites, located near Na^+ ions in supercages, and in 12-ring windows separating adjacent supercages, respectively. Simulation details can be found in Ref. [15].

1. Jump Diffusion or Molecular Dynamics?
2. Compute sites–barriers–rate constants ($\theta \rightarrow 0$)
 - Average T-site or explicit Si/Al in frame?
 - Zeolite rigid or flexible?
 - Guess or compute prefactors?
 - TST alone or TST with dynamical corrections?
3. Compute $D_g(\theta \rightarrow 0)$ from jumps–rate constants
 - Site lattice fixed or change with temp?
 - Analytical theory or kinetic Monte Carlo?
4. Compute loading-dependence of D_g
 - Site lattice fixed or change with loading?
 - Site blocking alone or blocking with attractions?
 - Analytical theory or kinetic Monte Carlo?

Figure 10: Model-building decisions for diffusion in zeolites; our choices underlined.

Below we give three main results: (i) three qualitative loading dependencies exhibited by the lattice model; (ii) the predicted loading dependence for benzene in NaX; (iii) novel adsorption and diffusion phenomena that arise when guest-guest attractions are large compared to thermal energies. The three loading dependencies that arise from our model when temperatures are relatively high are shown below in Figure 11. Alongside these loading dependencies are schematic cartoons that depict the physics of these transport systems. When the W and S_{II} site energies are thermally degenerate, adding additional molecules blocks sites and slows diffusion, hence giving Kärger and Pfeifer’s type I dependence. In the other extreme, adding additional molecules fills S_{II} site traps, which actually speeds up diffusion, giving Kärger and Pfeifer’s type IV dependence. At room temperature, we predict that type I will be found for benzene in

NaX, while type IV will be found for benzene in NaY. As discussed below, the former prediction agrees with PFG NMR data. However, the latter prediction is at odds with recent quasi-elastic neutron scattering data, which find a type I dependence for benzene in NaY [16].

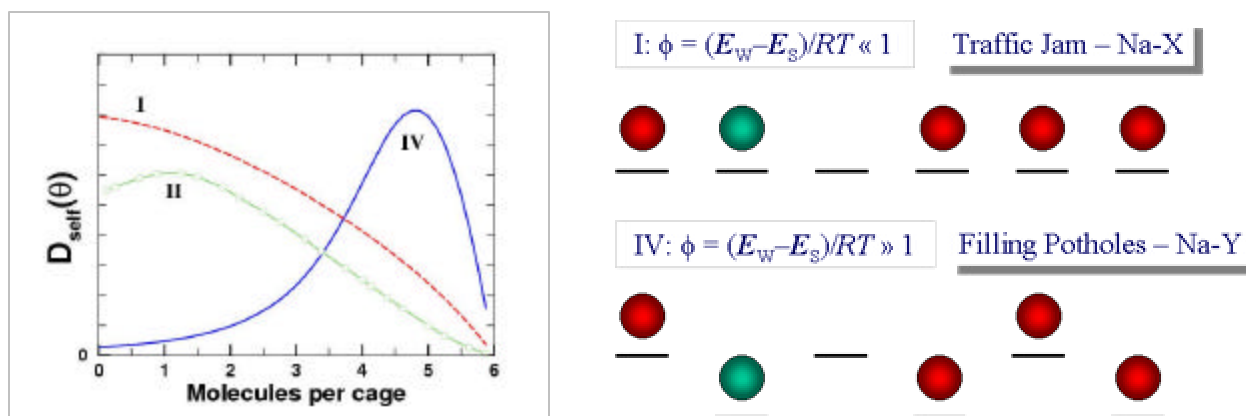


Figure 11: Loading dependencies of self-diffusion from lattice model, with corresponding cartoons.

Figure 12 shows simulation for benzene in NaX at $T = 393$ and 468 K, compared to PFG NMR data at the same temperatures (uniformly scaled by a factor of 5) [9], and TZLC diffusivities at $T = 468$ K (uniformly scaled by 100) [10]. Figure 12 shows that our model is in excellent qualitative agreement with PFG NMR, and in qualitative disagreement with TZLC. We suggest that high-temperature TZLC experiments should be performed, to test whether their type IV becomes a type I or II, as our simulations predict should happen.

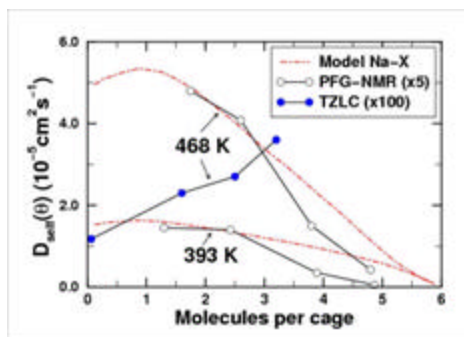


Figure 12: Comparing simulation, PFG NMR and TZLC for benzene in NaX.

We pause from these diffusion studies to wonder about the thermodynamic state of the confined fluid when guest-guest attractions become large compared to thermal energies. It is interesting to wonder whether fluids confined in nanopores can exhibit the analog of vapor-liquid equilibrium (VLE). The terms “vapor” and “liquid” are less meaningful for the adsorbed phase. Instead, we imagine a densification transition, whereupon a small increase in external sorbate pressure produces a precipitous increase in the sorbate loading. In adsorption experiments, the signature of this transition is hysteresis and capillary condensation, which are routinely observed for fluids confined in mesopores. However, for molecules in zeolites, these phenomena are much less common. This is not completely unexpected, since the critical temperature(s) for hysteresis and capillary condensation are expected to plummet as pore sizes approach molecular dimensions. The question is: can we find a zeolite-guest system for which this densification transition survives?

The likelihood of survival is increased when considering a guest phase with a large bulk VLE critical temperature, and a zeolite with relatively large cages. Here we consider benzene in NaX. Benzene has a bulk critical temperature of 562 K, and the NaX supercage is among the largest in zeolites. Saravanan and Auerbach performed grand canonical Monte Carlo simulations for benzene in NaX, using the lattice model derived for treating diffusion [17]. Figure 13 shows the resulting “coexistence curve,” alongside a cartoon depicting the transition from subcritical to supercritical states. We predict a densification critical temperature for benzene in NaX of *ca.* 370 K. This is lower than benzene’s bulk critical temperature, as expected, but is high enough to suggest that adsorption experiments may be able to observe hysteresis upon adsorption of benzene in NaX. (We note that hysteresis has been observed in adsorption isotherms measured for benzene in NaX [18]. However, this observation must arise from a structural transformation of the zeolite rather than from cooperative interactions among guests, because the measured densities in the adsorption branch *exceed* those in the desorption branch.)

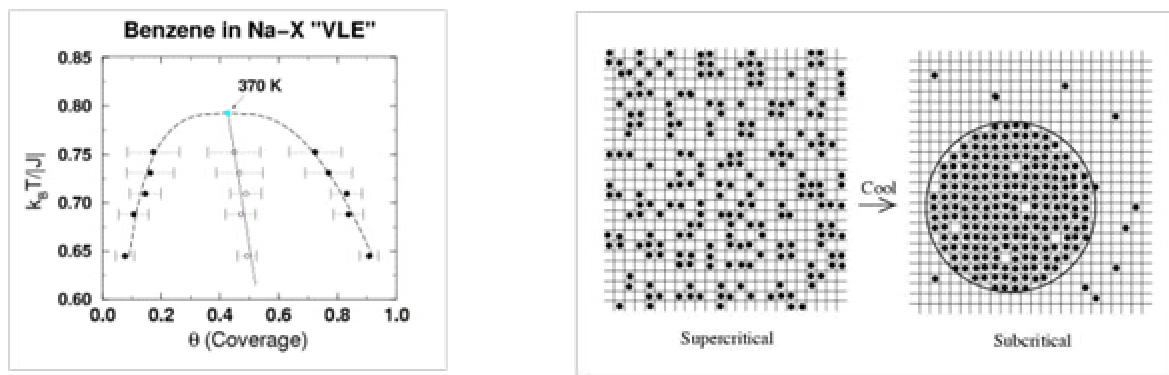


Figure 13: Simulation and schematic showing subcritical benzene in NaX.

We close this section by wondering what loading dependence of self-diffusion is expected for a subcritical adsorbed phase. Saravanan and Auerbach explored this by performing KMC simulations for analogs of benzene in NaX with various strengths of guest-guest attraction [15], all at $T = 468$ K. The results are shown in Figure 14. The systems with guest-guest attraction parameter $J = -2$ and -4 kJ/mol are supercritical, both showing a broadly decreasing loading dependence.

However, the system with $J = -7$ kJ/mol is in a subcritical state, and shows a qualitatively different loading dependence of self-diffusion. In particular, cluster formation in subcritical systems (see Figure 13) suggests a diffusion mechanism involving “evaporation” of particles from clusters. Increasing the loading in subcritical systems increases mean cluster sizes, and smoothes cluster interfaces. Once these interfaces become sufficiently smooth, we surmise that evaporation dynamics remain essentially unchanged by further increases in loading. As such, we expect the subcritical diffusivity to obtain its full loading value at low loadings, and then remain roughly constant up to full loading, as seen in Figure 14.

This type of loading dependence, involving broad regions of constant diffusivity, is surprising, since isotherms for interacting sorbates are expected to decrease with loading when site blocking dominates. This loading dependence is essentially the same as Kärger and Pfeifer’s type III, which is observed for strongly associating fluids such as water and ammonia in NaX. This analysis suggests that Kärger and Pfeifer’s type III loading dependence may be characteristic of a cluster-forming, subcritical adsorbed phase.

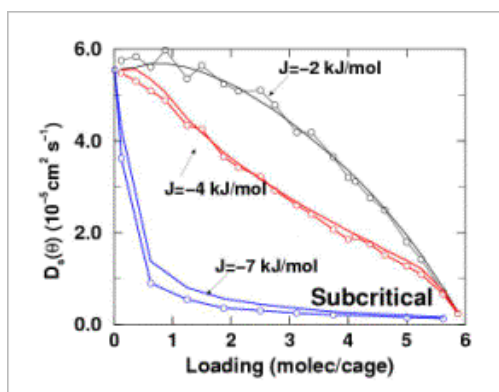


Figure 14: Predicted loading dependencies of subcritical and supercritical fluids in zeolites.

6. Concluding Remarks

Jump diffusion models have significantly elucidated transport in zeolites. Here we have seen how defects in zeolites, single-file diffusion, zeolite flexibility, host-guest interactions and phase transitions influence the temperature and loading dependencies of diffusion in zeolites. Despite this initial progress, much work remains. In particular, recent PFG NMR data suggests strongly that zeolites are not the ordered frameworks we surmise them to be [19]. A major challenge for future zeolite scientists is thus developing models that retain the beautiful atomic structure of zeolites, while incorporating realistic representations of disorder present in real materials. Progress along these lines should feature prominently at future NATO Advanced Study Institutes on Fluid Transport in Nanopores.

7. Acknowledgments

I thank Profs. J. Fraissard, W.C. Conner, Jr., and V. Skirda for the invitation to speak at and write for the NATO Advanced Study Institute. I thank them also for partially funding my trip. I thank all my previous and present coworkers for their invaluable efforts toward revealing the fascinating world of fluid transport in nanopores. But mostly, I thank my wife Sarah for taking care of the kids while I write this.

References:

1. Nelson, P.H., M. Tsapatsis, and S.M. Auerbach, *Modeling Permeation Through Anisotropic Zeolite Membranes with Nanoscopic Defects*. J. Membrane Sci., 2001. **184**: p. 245-255.
2. Levitt, D.G., Phys. Rev., 1973. **A8**: p. 3050.
3. Nelson, P.H. and S.M. Auerbach, *Self Diffusion in Single-File Zeolite Membranes is Fickian at Long Times*. J. Chem. Phys., 1999. **110**: p. 9235-9243.
4. Hahn, K. and J. Karger, J. Phys. Chem. B, 1998. **102**: p. 5766.
5. Snurr, R.Q., A.T. Bell, and D.N. Theodorou, J. Phys. Chem., 1994. **98**: p. 11948.
6. Forester, T.R. and W. Smith, *Bluemoon Simulations of Benzene in Silicalite-1: Prediction of Free Energies and Diffusion Coefficients*. J. Chem. Soc., Faraday Trans., 1997. **93**: p. 3249-3257.
7. Turaga, S.C. and S.M. Auerbach, *Calculating Free Energies for Diffusion in Tight-Fitting Zeolite-Guest Systems: Local Normal-Mode Monte Carlo*. J. Chem. Phys., 2003. **118**: p. 6512-6517.
8. Iyer, K.A. and S.J. Singer, *Local-Mode Analysis of Complex Zeolite Vibrations: Zeolite A*. J. Phys. Chem., 1994. **98**: p. 12679-12686.
9. Germanus, A., et al., Zeolites, 1985. **5**: p. 91.
10. Brandani, S., Z. Xu, and D. Ruthven, Microporous Materials, 1996. **7**: p. 323-331.
11. Auerbach, S.M., *Theory and Simulation of Jump Dynamics, Diffusion and Phase Equilibrium in Nanopores*. Int. Rev. Phys. Chem., 2000. **19**: p. 155-198.
12. Auerbach, S.M., F. Jousse, and D.P. Vercauteren, *Dynamics of Sorbed Molecules in Zeolites*, in *Computer Modelling of Microporous and Mesoporous Materials*, B. Smit, Editor. 2003, Academic Press: London.
13. Karger, J., S. Vasenkov, and S.M. Auerbach, *Diffusion in Zeolites*, in *Handbook of Zeolite Science and Technology*, P.K. Dutta, Editor. 2003, Marcel Dekker, Inc.: New York. p. 341-422.
14. Karger, J. and H. Pfeifer, Zeolites, 1987. **7**: p. 90.
15. Saravanan, C. and S.M. Auerbach, *Theory and Simulation of Cohesive Diffusion in Nanopores: Transport in Subcritical and Supercritical Regimes*. J. Chem. Phys., 1999. **110**: p. 11000-11010.
16. Jobic, H., A.N. Fitch, and J. Combet, *Diffusion of benzene in NaX and NaY zeolites studied by quasi-elastic neutron scattering*. J. Phys. Chem. B, 2000. **104**: p. 8491-8497.
17. Saravanan, C. and S.M. Auerbach, *Simulations of High T_c Vapor-Liquid Phase Transitions in Nanoporous Materials*. J. Chem. Phys., 1998. **109**: p. 8755-8758.
18. Tezel, O.H. and D.M. Ruthven, J. Coll. Inter. Sci., 1990. **139**: p. 581.
19. Vasenkov, S., et al., *PFM NMR Study of Diffusion in MFI-type Zeolites: Evidence of the Existence of Intracrystalline Transport Barriers*. J. Phys. Chem. B, 2001. **105**: p. 5922-5927.